Electrochemical characterization of innovative hybrid coatings for metallic artefacts

(Article begins on next page)

19 April 2024

Electrochemical characterization of innovative hybrid coatings for metallic artefacts

Leonardo Iannucci
Dipartimento di Elettronica e Telecomunicazioni, Politecnico di Torino, Torino, Italy

J. F. Ríos-Rojas
Universidad Antonio Nariño, Grupo de Investigación REM-Research in Energy and Materials, Bogotá, Colombia

Emma Angelini
Dipartimento di Scienza Applicata e Tecnologia, Politecnico di Torino, Torino, Italy

Marco Parvis
Dipartimento di Elettronica e Telecomunicazioni, Politecnico di Torino, Torino, Italy

Sabrina Grassini
Dipartimento di Scienza Applicata e Tecnologia, Politecnico di Torino, Torino, Italy

Electrochemical characterization of innovative hybrid coatings for metallic artefacts

L. Iannucci[1], J. F. Ríos-Rojas[2], E. Angelini[3], M. Parvis[1], and S. Grassini[3]

[1] Politecnico di Torino, Dipartimento di Elettronica e Telecomunicazioni, Torino, Italy
[2] Universidad Antonio Nariño, Grupo de Investigación REM-Research in Energy and Materials, Bogotá, Colombia
[3] Politecnico di Torino, Dipartimento di Scienza Applicata e Tecnologia, Torino, Italy

Abstract. In this paper, an electrochemical characterization of two different hybrid coatings is presented, with the specific aim of studying their corrosion protection behavior and better understanding their possible application in the cultural heritage field. The two formulations under study were epoxy resin containing silica nanoparticles and epoxy resin containing graphene oxide. Electrochemical Impedance Spectroscopy (EIS) and Scanning ElectroChemical Microscopy (SECM) were used to compare the electrochemical behavior of the two coatings and highlight their failure mechanism when immersed in an electrolytic solution containing chlorides. The investigation highlighted the good corrosion protective properties of both coatings; and moreover, thanks to the joined use of the two described analytical techniques, the different water uptake of the two solutions was studied, together with the different evolution of the coating surface morphology when immersed in the electrolytic solution.

PACS. 81.65.Kn Corrosion protection – 81.07.Pr Organic-inorganic hybrid nanostructures

1 Introduction

Protection of metallic artefacts from corrosion is a multifaceted issue which requires different expertises, from the design of new coatings to the use and development of technologies to apply innovative materials and techniques to characterize them. Often the solution is represented by a coating able to act as a barrier against external environment and aggressive agents, but in the cultural heritage field, many constraints are present in the choice of the best system to protect an artefact from degradation. Actually, the coating performance itself is only one of the parameters that have to be considered. As an example, visual appearance (e.g. transparency) is fundamental, in order to not alter the artwork and moreover, it has to be considered that the coating should have a good adherence not only on bare metal, but also on oxides or corrosion products that could be present on the surface of the artefact. Then, also long term efficiency, easiness of maintenance and coating reversibility have to be taken in account [1]. Because of all these reasons, research is always active in this field in order to find out innovative and better performing solutions.

Several are the commonly used products in the conservation of cultural heritage metallic artefacts, but they can be clustered into three main categories: varnishes, waxes and corrosion inhibitors [2]. In a survey carried out between museum curators of different countries of the Mediterranean basin, it was shown that the most commonly used coatings are acrylic resins (such as Paraloid™ B-72, a copolymer of ethyl methacrylate and methyl methacrylate) and microcrystalline waxes [3]. The major problems that could arise with these materials are mainly due to either the presence of localized corrosion phenomena, in case of poor adhesion at the metal-coating interface, or a limited long-term stability, especially in the case of waxes. Moreover, few are the products that are able to withstand harsh environmental conditions, such as those encountered by the artefacts that are exposed outside of museums. In this case, barrier properties against water and moisture, UV-rays resistance and long term stability become crucial. In these conditions, an innovative possibility which might be used for the protection of metallic artefacts from corrosion could be represented by hybrid polymeric coatings [4]. This is a new class of materials with tailored properties which are in between of those of organic and inorganic materials. In this research work, the attention is focused on polymer/silica hybrid nanocoatings and graphene oxide epoxy coatings. In the first case, nanometric silica domains are immersed inside a polymeric matrix (epoxy resin) [5]; the result is a material that combines toughness and surface properties typical of polymers with hardness, chemical and thermal stability typical of inorganic glasses [6]. Different studies demonstrated the improvement in scratch resistance and barrier properties to gases (compared to the bare polymer), still keeping

the transparency [7]; all these characteristics make this material a suitable choice in the protection of cultural heritage pieces. The second case is represented by epoxy coatings containing graphene oxide, a lamellar nanofiller which is dispersed inside the polymeric matrix, leading to improvements (from the barrier properties and hardness point of view) similar to those of silica-based hybrid coatings [8]. The main advantage of graphene oxide coatings is the extremely low filler content, that is beneficial also for the visual appearance. Based on these considerations hybrid polymeric coatings, whose compatibility and reversibly are most similar to those of epoxy-based resins, but whose protective effectiveness is higher, can be suitable new materials for the preservation of metallic artefacts.

In this paper, a comparison of silica-based and graphene oxide-based hybrid coatings has been carried out; their corrosion protection performance has been estimated by means of Electrochemical Impedance Spectroscopy (EIS) and Scanning Electro-Chemical Microscopy (SECM), with the specific aim of comparing the information given by these two techniques and better understand also the coating failure mechanism. EIS is nowadays an electrochemical technique widely used also in the cultural heritage field to assess the protective effectiveness of coatings [9–11]. Main EIS advantages are related to the possibility to perform the measurements through a very low signal. In this way, corrosion of the metallic substrate is not accelerated by the polarization applied [12,13]. At the same time, one of the main limits of EIS is that the measurements are usually performed on a large surface area, so the result may be affected by the presence of small defects in the polymeric film. A small leak can drastically reduce the measured impedance, even though the overall behavior of the coating is still good. In order to overcome this intrinsic limitation, the characterization has been carried out also by means of SECM. In this case, a micro-probe scans the sample surface detecting oxidation reactions that are in progress [14]. A variation in the current profile measured by the instrument is a clue of degradation of the protective coating. In this way, single small defects can be detected and the coating electrochemical behavior can be monitored as a function of the immersion time in the electrolytic solution. More precise information on the degradation mechanism can be obtained [15,16], in particular from the point of view of morphological modifications of the surface and early stages of coating deterioration.

2 Materials and methods

In order to test the characteristics of the two coating families, low carbon steel Q-Panel Standard Test Substrate, purchased from Q-Lab, were used as coated material. These substrates have a superficial roughness $R_a = 0.5$ μm, as declared in the product specifications. The Q-Panel substrates were cut to the dimensions of 25 mm $\times$ 25 mm and then cleaned with acetone.

Two coatings have been studied: epoxy resin filled with TEOS (Tetraethoxysilane - 15 wt%) and epoxy resin filled with graphene oxide (0.05 wt%). Bare epoxy coatings were prepared for comparison by using 3,4-epoxycyclohexylmethyl - 3',4-epoxycyclohexyl carboxylate (CE) purchased from Sigma-Aldrich. All polymeric films were photocured and Irgacure 250 (Basf) was used as photoinitiator (concentration 4 wt% respect to the epoxy resin).

Samples coated with the TEOS formulation underwent a heat treatment to complete the sol-gel reactions (90° C for 4 hours at 95% RH) following the procedure presented in [17]. Graphene oxide was dispersed in the resin using IKA Ultra-turrax at 30000 rpm for about 5 min and finally placing the mixture in an ultrasonic bath for about 60 min, as described in [18].

Formulations were deposited on the steel substrates using the draw-down rod coating technique in order to obtain a fixed and controlled thickness of about 60 μm $\pm$ 15 μm. The used procedure is the same described in other research papers [19,20]: some coating liquid is placed on the substrate surface, afterwards a wire wound rod is rolled over the surface, so as to spread the liquid over the whole surface and doctor off the excess of coating fluid. Any other deposition technique could be applied (e.g. brushing, spraying etc.), but the draw-down rod technique assures an easy and reproducible procedure. UV-curing process was the following step and had a duration of about 120 s with light irradiance on the sample surface of about 60 mW/ cm^2.

Coated samples were characterized by means of EIS and SECM in order to investigate their corrosion behavior. EIS measurements were performed in a conventional three electrodes electrochemical cell filled with 0.1 M NaCl (sodium chloride) aerated solution. An Ag/AgCl electrode was used as the reference electrode and a NiCr wire as the counter electrode. Measurements were performed in the range of 0.01 Hz to 100 kHz, with an applied voltage of 100 mV$_{pp}$ to stress the coating similarly to the SECM analysis described below. The exposed area was of about 0.8 cm^2; all results have been scaled to the equivalent area of 1 cm^2. Measurements were performed every 24 hours for 5 days in order to understand the protective effectiveness of the coating exposed to the aggressive solution.

SECM analyses were carried out in 0.1 M KCl (potassium chloride), to which 5 mM K$_4$Fe(CN)$_6$ $\cdot$ 3H$_2$O (potassium ferrocyanide) solution was added to act as electrochemical mediator. The measuring cell was composed of a tip with diameter of 10 μm (set as working electrode), a reference electrode (Ag/AgCl electrode) and a counter electrode (Pt wire). The tip was positioned at a distance of 10 μm (equal to the tip diameter) from the sample surface. This was detected with a vertical line-scan in feedback mode as the height at which a 25% reduction of the current was measured by the probe respect to the value in bulk solution. Acquisitions were performed through a scan rate of 30 μm/s and a step size of 10 μm. The tip was set at a potential of +0.5 V with respect to the Ag/AgCl reference electrode; the
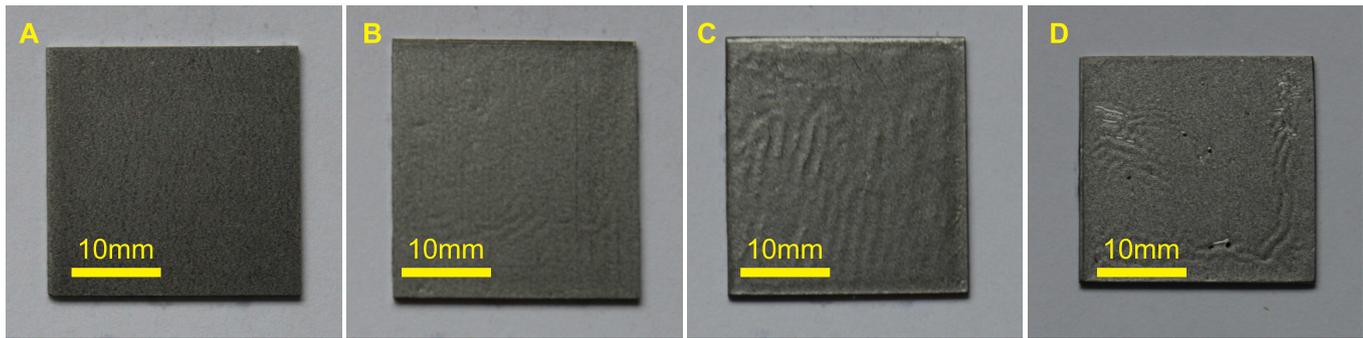
Fig. 1: Samples under study: A) Steel B) Epoxy Coating C) Epoxy-TEOS Coating D) Graphene Oxide Coating

current that is measured between working and counter electrodes is due to two possible oxidation reactions inside the solution related to the electrochemical mediator (eq. 1) and to the corrosion reaction of the steel substrate (eq. 2), respectively:

$$Fe(CN)_6^{4-} \longleftrightarrow Fe(CN)_6^{3-} + e^- \tag{1}$$

$$Fe^0 \longrightarrow Fe^{2+} + 2e^- \tag{2}$$

Being that the sample is non-conductive, as long as the coating covers and protects the surface, the only signal is given by the mediator oxidation reaction (eqn. 1). Thus the value of current that is measured depends on the distance between the tip and the sample surface: approaching the surface, oxidation reactions are limited by hindered diffusion of new species near the tip, so the measured current decreases. The SECM measurements, performed on areas of $500 \ \mu m \times 500 \ \mu m$, were used to obtain morphological information about samples surface.

The morphological characterization was performed by means of a Field Emission Scanning Electron Microscope (FESEM Supra 40, ZEISS) using 15 kV and and aperture of 20 μm to take high magnification images.

3 Results and discussion

Visual appearance of the coated samples can be observed in Fig. 1. All coatings show a good transparency; the finishing is slightly glossy, but it does not modifies the aesthetic appearance of the metallic substrate. The use of a draw-down rod for coating deposition allows one to obtain a constant thickness, but turns out in a not perfectly flat coating which sometimes appears as a wavering on the images. However this drawback can be easily overcome when the coating is applied onto a real artefact, thanks to the high adaptability of the epoxy-based coating to any surface roughness.

As described in other works [5], the microstructure of Epoxy-TEOS hybrid coatings is characterized by the presence of a nanometric silica phase, which does not alter the transmission of visible light, i.e. it does not change the surface color. Similarly, the graphene oxide addition to the epoxy resin is rather limited so that also in this case no color change is expected. The color difference C_d between the different coated samples can be expressed as:

$$C_d = \frac{\sqrt{\delta R^2 + \delta G^2 + \delta B^2}}{L} \tag{3}$$

where δR, δG, δB are the color difference of each average color component with respect to the bare Q-panel and L is the average lightness of each sample. When the reflectivity effect is removed (i.e. when the different images have been scaled to have the same L) the color difference C_d is of about 1% for Epoxy-TEOS Coating, 0.5% for the Graphene Oxide Coating and 1.5% for the Epoxy Coating without any filler addition.

Fig. 2 shows the FESEM micrographs of the Epoxy-TEOS coating before and after 96h of immersion in the NaCl solution. The same morphology described in literature for Epoxy-TEOS coatings can be observed. Some silica nanoparticles, characterized by size in the range of $100 - 200$ nm, are visible near the surface of the coating already after deposition. Actually, this can be explained because the inorganic phase (more polar than the organic one) tends to enrich superficial layers of the material. After permanence inside the electrochemical cell, a slight degradation of the resin occurs and it leads to the exposure of silica nanoparticles directly to the surface. The nanoparticles appear well distributed and dispersed in the organic matrix, without a major segregation of the silica phase. In the case of graphene oxide coatings, shape and dimension of the filler made impossible to distinguish it inside the matrix. This can also be interpreted as a sign of good dispersion of the nanofiller inside the polymer.

Electrochemical Impedance Spectroscopy (EIS) was the first characterization technique that was used in order to study the barrier properties of the coatings. Results are reported in Fig. 3 as Bode diagrams. As it can be observed,
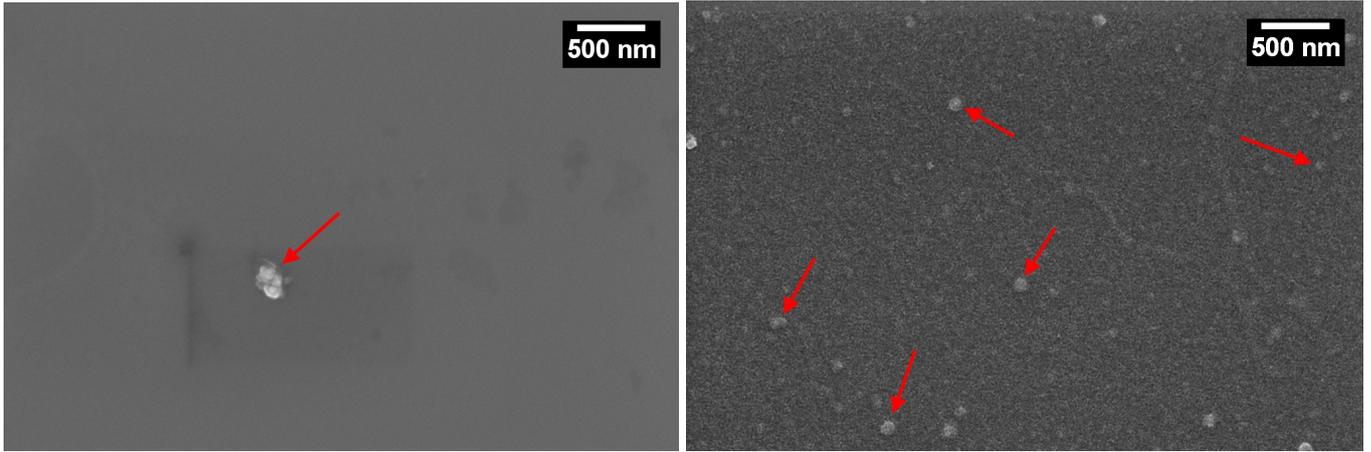
Fig. 2: FESEM micrographs of the Epoxy-TEOS coating as deposited (on the left) and after 96 hours of immersion in 0.1 M NaCl aerated solution in the electrochemical cell used for the EIS measurements (on the right)
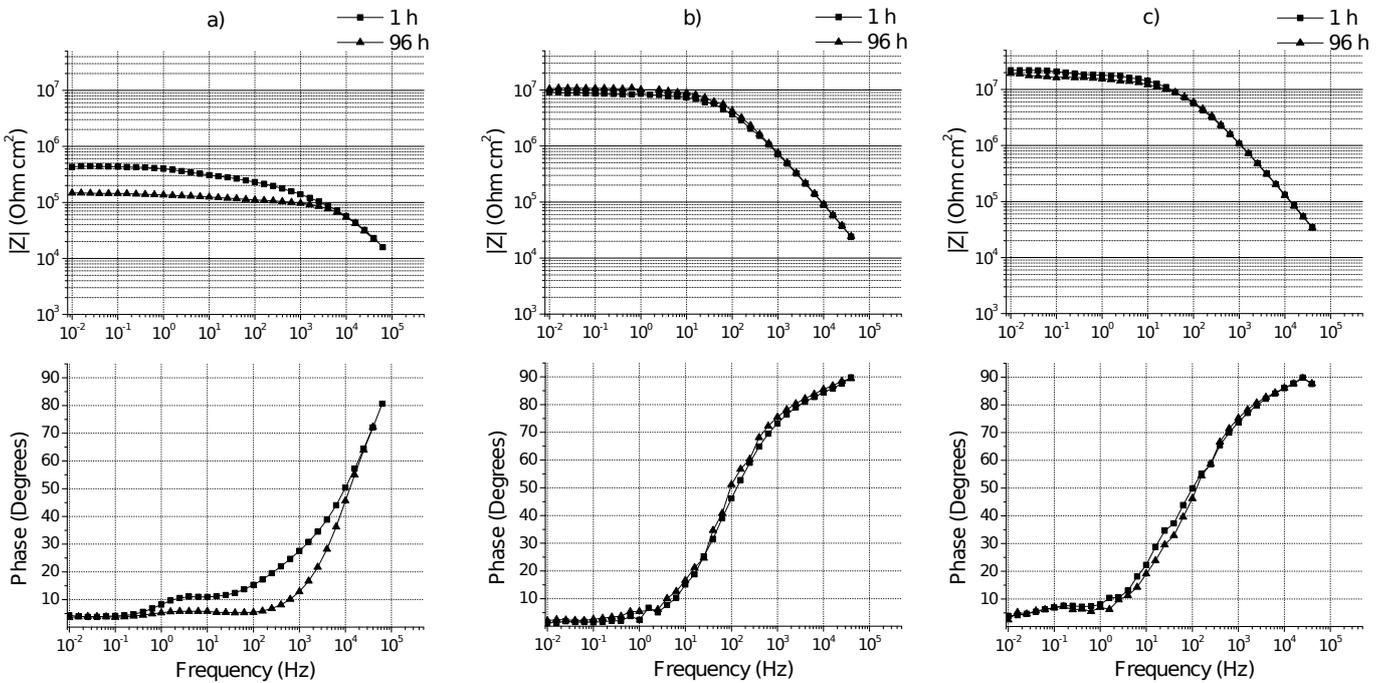

Fig. 3: Bode plots recorded on a) Epoxy Coating, b) Epoxy-TEOS Coating and c) Graphene Oxide Coating after 1 hour and 96 hours of immersion in the 0.1 M NaCl aerated solution

all samples show a stable electrochemical behavior during the 96 hours of immersion in the NaCl aggressive solution. For both hybrid coatings $|Z|$ reaches values of about $10^7 \ \Omega \cdot \text{cm}^2$ or above at low frequencies, highlighting a good protective effectiveness of the Epoxy-TEOS and Graphene Oxide coatings towards the corrosion of the steel substrate.

The bare Epoxy Coating, instead, has an impedance modulus of more than one order of magnitude lower than the hybrid coatings, highlighting the importance of the nanofillers to improve the protective effectiveness of the epoxy resin. Measurement results have been modeled through the equivalent circuit model shown in Fig.4, typically used in the case of organic coatings that undergo a degradation, where R_s is the resistance of the electrolytic solution which has been assumed fixed at the value of 150 Ω, R_f is the film resistance, in parallel with CPE_{Cf} (a Constant Phase Element) representing the capacitance of the film and eventually R_{ct} is the Charge Transfer resistance, in parallel with another CPE (CPE_{Cdl}), that models the double layer capacitance at the interface with the metal.
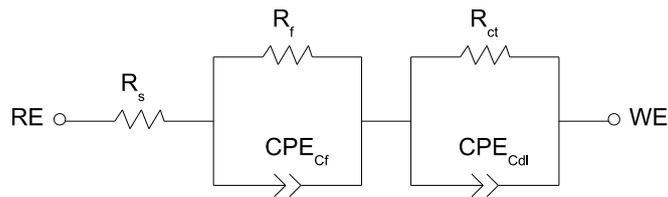
Fig. 4: Equivalent circuit model used for fitting the EIS spectra of Fig. 3

Table 1: R_{ct} and CPE_{Cdl} values obtained by fitting the impedance spectra by the equivalent circuit model of Fig. 4

	R_{ct} ($\Omega \cdot cm^2$) 1 hour	CPE_{Cdl}, 1 hour		R_{ct} ($\Omega \cdot cm^2$), 96 hours	CPE_{Cdl}, 96 hours	
Epoxy	3.08×10^5	4.14×10^{-7}	$(\alpha = 0.7)$	1.40×10^5	2.66×10^{-6}	$(\alpha = 0.7)$
Epoxy-TEOS	1.09×10^7	3.82×10^{-6}	$(\alpha = 0.7)$	1.20×10^7	8.23×10^{-8}	$(\alpha = 0.8)$
Graphene Oxide	2.39×10^7	3.32×10^{-7}	$(\alpha = 0.8)$	1.94×10^7	3.64×10^{-7}	$(\alpha = 0.7)$
Low Carbon Steel	3.56×10^2	2.64×10^{-3}	$(\alpha = 0.8)$			

The physical meaning of the CPE in the equivalent circuit model is correlated to the surface heterogeneity of the coatings [21,22]; the CPE impedance value is represented by equation:

$$Z = \frac{C}{(i \cdot \omega)^\alpha} \tag{4}$$

where C is a constant related to the specific system under investigation, $\omega = 2\pi f$ takes into account the frequency, $i = \sqrt{-1}$ is the imaginary unit and α is a coefficient independent from frequency that ranges between 0 and 1 [21]. This element is a generalization of a classic capacitor, which becomes a specialized case of a CPE, when $\alpha = 1$; when $\alpha = 0$ the CPE is equivalent to a resistor, while when $\alpha = $ -1 is equivalent to an inductor.

R_{ct} and CPE_{Cdl} values obtained by fitting the EIS spectra by means of the equivalent circuit model of Fig.4 are reported in Table 1. For the steel sample, R_{ct} is of about 350 $\Omega \cdot cm^2$ and CPE_{Cdl} is of about $2.64 \cdot 10^{-3}$ with $\alpha = 0.8$, thus indicating the poor corrosion resistance of the low carbon steel in the aggressive electrolyte. A significant increase in the charge transfer resistance can be observed for the two hybrid coatings with respect to the bare metal, but also when compared to the bare Epoxy Coating. Moreover, during the 96 hours of exposure to the electrolytic solution, no significant changes could be observed for the Epoxy-TEOS and Graphene Oxide coatings, while the resistance to charge transfer decreases for the Epoxy Coating.

From the fitting of the impedance spectra, α values close to the unity were obtained for all samples, indicating a behavior similar to a capacitor. High values of the CPE_{Cdl} are expected for bare low carbon steel substrates, while lower values are recorded onto coated samples not affected by degradation. Moreover, such CPE values remain almost constant for the Graphene Oxide Coating over the 96 hours of exposure inside the electrochemical cell, while the value increases for the Epoxy Coating without filler. Eventually, the CPE_{Cdl} value decreases for the Epoxy-TEOS probably due to the water uptake by the coating exposed to the electrolytic solution.

In agreement with EIS measurements, no signs of corrosion could be observed on the metallic surface and the metal was still coated by the polymeric coatings, as confirmed by the FESEM analysis. Only a slight degradation of the epoxy resin could be observed, as it can be seen in Fig. 2 for the Epoxy-TEOS sample.

In order to better understand the degradation mechanism of the different coatings when immersed in the electrolytic solution, the SECM technique was used. The same area was scanned at different immersion times, in order to detect changes in its roughness or defects being formed. Results for Epoxy-TEOS and graphene oxide samples are presented in Fig. 5.

SECM graphs have been plotted with the z axis (representing the current) inverted, so as to give a direct topographical representation of the surface. Specimens appear not perfectly flat since the beginning of the test, due to the manual procedure to spread the coating on the metal surface. Epoxy-TEOS specimens show a higher roughness (respect to grafene oxide samples), characterized by peaks that protrude from the surface. Moreover, this kind of defects increase their dimension with the immersion time in the electrolyte, even if this does not influence the protective capabilities of the coating (as seen through the EIS measurements). The reason for this changes can be attributed to water uptake by the polymer, discovered in an early stage through SECM technique, but still difficult to detect through EIS. Actually, in order to have a significant decrease in the impedance modulus, a longer ionic conductive path would be necessary, so longer immersion time are required. In the case of graphene oxide coatings, the surface is smoother, even if still characterized by the presence of peaks. A notable point is that in this case the surface is less
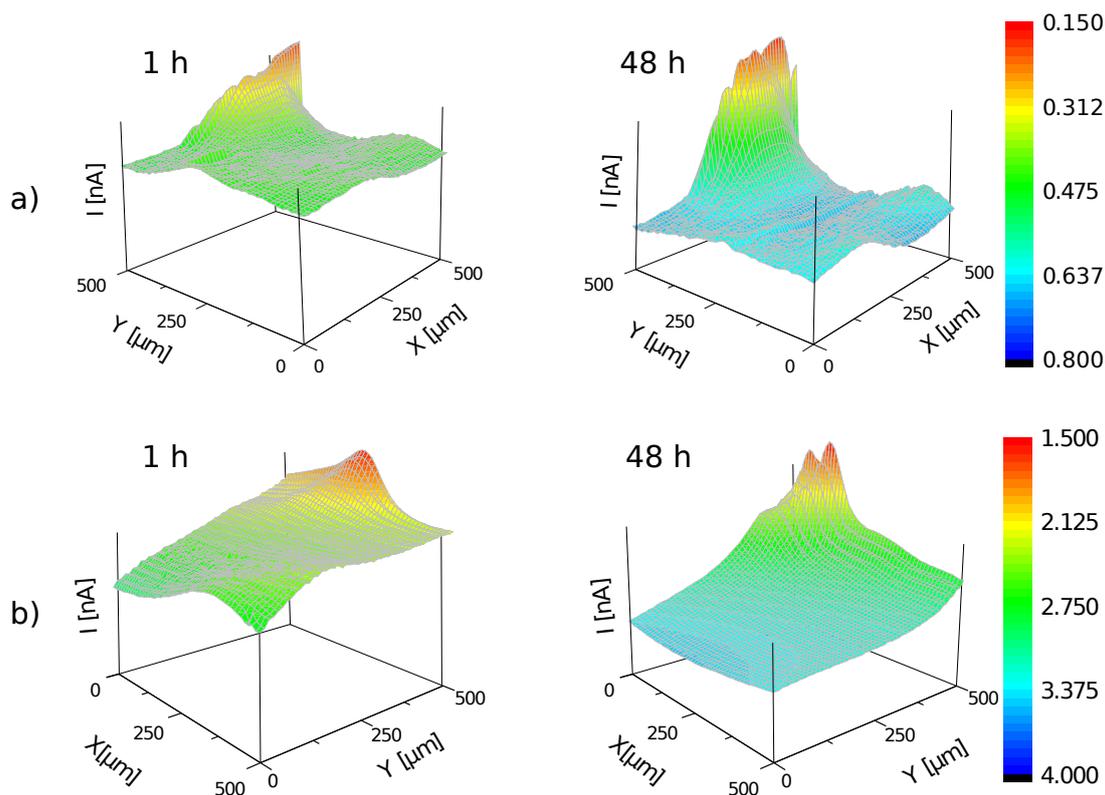
Fig. 5: SECM measurement on a) Epoxy-TEOS and b) Epoxy-Graphene Oxide coatings after 1 hour and 48 hours

deteriorated by the immersion in the electrolytic solution, both considering the peaks and the mean roughness of the surface.

This behavior can be explained in a twofold way. First of all, the shape of the filler inside the polymeric matrix plays an important role, as the lamellar shape of graphene oxide nanoplatelets is particularly suited to obstacle the diffusion of electrolyte through the coating [23,24]. Actually, as it can be seen also from FESEM micrographs, silica nanoparticles have a spherical shape, which leads to lower tortuosity if compared to the effect of lamellar fillers [25]. Moreover, also the different hydrophilicity of the two coatings must be taken in account. As reported in scientific literature for analogous materials, TEOS-containing coatings are characterized by lower contact angles with water respect to graphene oxide ones [17,18]. The role of the filler, if compared to graphene oxide coatings, is less effective in preventing absorption of water from the environment. Thus SECM measurements are an additional evidence of the different behavior of the two materials, which is in good agreement with previous literature [7,26].

4 Conclusions

A comparative characterization of two different hybrid coatings has been presented in this paper. The characteristics of these two coatings, such as transparency, superficial hardness, gas barrier properties and easiness of preparation, make them interesting materials for protection of metallic artefacts from degradation. Moreover, being both photocured coatings, their preparation does not involve the use of organic solvents or high temperature that could be detrimental for the artefacts, and in the case of the Graphene Oxide loaded coating all the process is carried out at room temperature therefore avoiding any thermal stress to the artefact. Results from electrochemical impedance spectroscopy have shown for both TEOS and Graphene Oxide loaded coatings good corrosion protective properties, also after one week of exposure to a solution containing aggressive chloride ions.

Measurements performed through SECM permitted to study more in-depth the failure mechanism of the coatings, highlighting a significant water uptake by TEOS-containing coatings that was discovered also through EIS. This behavior can be explained thanks to the higher hydrophilicity of Epoxy-TEOS coatings respect to graphene oxide ones. Because of this, the Graphene Oxide loaded coated samples appear to have a more stable behavior, suitable for a long-term protection of metallic artefacts. In addition, the coating procedures for the graphene loaded resin, which is carried out at room temperature, makes it an excellent choice for the ancient artefacts.

5 Acknowledgements

References

1. Dillmann, P., Beranger, G., Piccardo, P., Matthiesen, H., *Corrosion of metallic heritage artefacts* (Woodhead Publishing, Cambridge 2007) pp 308-314
2. Dillmann, P., Watkinson, D., Angelini, E., Adriaens, A., *Corrosion and Conservation of Cultural Heritage Metallic Artefacts* (Woodhead Publishing, Cambridge 2013).
3. Argyropoulos, V., Giannoulaki, M., Michalakakos, G.P., Siaotou, A., *Proceedings of the International Conference on Conservation Strategies for Saving Indoor Metallic Collections, Cairo 25 February - 1 March 2007* (TEI of Athens, Athens 2007) pp 166-170.
4. Zheng, S., Li, J., J Sol-Gel Sci Technol **54**, (2010) pp. 174-187.
5. Amerio, E., Sangermano, M., Malucelli, G., Priola, A., Voit, B., Polymer **46**, (2005) pp. 11241-11246.
6. Torrico, R., Harb, S.V., Trentin, A., Uvida, M.C., Pulcinelli, S.H., Santilli, C.V., Hammer, P., Journal of Colloid and Interface Science **513**, (2018) pp. 617-628.
7. Sangermano, M., Malucelli, G., Amerio, E., Priola, A., Billi, E., Rizza, G., Progress in Organic Coatings **54**, (2005) pp. 134-138.
8. Kausar, A., Rafique, I., Anwar, Z., Muhammad, B., Polymer-Plastics Technology and Engineering **55:7**, (2016) pp. 704-722.
9. Cano, E., Lafuente, D., Bastidas, D. M., J Solid State Electrochem **14**, (2010) pp. 381-391.
10. Angelini, E., Grassini, S., Parvis, M., Zucchi, F., Surf. Interface Anal. **44**, (2012) pp. 942-946.
11. Grassini, S., Angelini, E., Parvis, M., Bouchar, M., Dillmann, P., Neff, D., Appl Phys A **113**, (2013) pp. 971-979.
12. Amirudin, A., Thierry, D., Progress in Organic Coatings **26**, (1995) pp. 1-28.
13. Grassini, S., Corbellini, S., Parvis, M., Angelini, E., Zucchi, F., Measurement **114**, (2018) pp. 508-514.
14. Sun, P., Laforge, F. O., Mirkin, M. V., Physical Chemistry Chemical Physics **9**, (2007) pp. 802-823.
15. Souto, R.M., Gonzlez-Garca, Y., Gonzlez, S., Progress in Organic Coatings **65**, (2009) pp. 435-439.
16. Souto, R.M., Gonzlez-Garca, Y., Izquierdo, J.,Gonzlez, S., Corrosion Science **52**, (2010) pp. 748-753.
17. Amerio, E., Sangermano, M., Malucelli, G., Priola, A., Billi, E., Rizza, G., Macromolecular Materials and Engineering **291**, (2006) pp. 1287-1292.
18. Periolatto, M., Di Francia, E., Sangermano, M., Grassini, S., Russo Spena, P., *Advanced Epoxy-Based Anticorrosion Coatings Containing Graphene Oxide* (Springer International Publishing, 2017) pp 135-143.
19. Meng, Y., Xu, X.-B., Li, H., Wang, Y., Ding, E.-X., Zhang, Z.-C., Geng, H.-Z-, Carbon **70**, (2014) pp. 103-110.
20. Dan, B., Irvin, G.C., Pasquali, M., ACS Nano **3**, 4, (2009) pp. 835-843.
21. Kahanda, G. L. M. K. S., Tomkiewicz, Micha, J. Electrochem. Soc. **137**, (1990) pp. 3423-3429.
22. Barsoukov, E., Ross Macdonald, J., *Impedance Spectroscopy: Theory, Experiment, and Applications* (Wiley, 2005)
23. Hayatgheib, Y., Ramezanzadeh, B., Kardar, P., Mahdavian, M., Corrosion Science **133**, (2018) pp. 358-373.
24. Zheng, H., Guo, M., Shao, Y., Wang, Y., Liu, B., Meng, G., Corrosion Science **139**, (2018) pp. 1-12.
25. Bharadwaj, R. K., Macromolecules **34**, (2001) pp. 9189-9192.
26. Sangermano, M., Periolatto, M., Signore, V., Russo Spena, P., Progress in Organic Coatings **103**, (2017) pp. 152-155.